

Rearrangement of the Active Ester Intermediate During HOBt/EDC Amide Coupling

Khaled A. Mahmoud,^[a] Yi-Tao Long,^[a] Gabriele Schatte,^[b] and Heinz-Bernhard Kraatz^{*[a]}

Keywords: Ferrocene / Hydroxybenzotriazole / Amide coupling / Amino acid / Electrochemistry

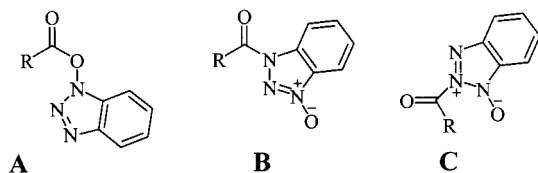
3-[[1'-(*tert*-Butyloxycarbonylamino)ferrocen-1-yl]carbonyl]-benzotriazole 1-oxide (**3**) has been successfully separated during the synthesis of benzotriazol-1-yl 1'-(*tert*-butyloxycarbonylamino)ferrocene-1-carboxylate (**2**) as an active ester for peptide coupling. The yield of **3** increased by using polar, rather than nonpolar solvents. The two compounds have been fully characterized and studied by X-ray crystallography and spectroscopic methods. The active ester derivative **2** formed a urethane bond with the glycine ethyl ester while the *N*-oxide **3** did not react. The X-ray structural ana-

lysis of **3** shows strong intermolecular hydrogen bonding involving the urethane group and the *N*-oxide of an adjacent molecule [$N\cdots H-N = 2.859(2) \text{ \AA}$]. No hydrogen bonding is present in the solid state for compound **2**, while solution studies indicate the presence of intramolecular hydrogen bonding. Both complexes display a quasi-reversible single one-electron oxidation, the halfwave potentials $E_{1/2}$ for **2** and **3** were 672 ± 5 and 591 ± 5 mV, respectively.

(© Wiley-VCH Verlag GmbH & Co. KGaA, 69451 Weinheim, Germany, 2005)

Introduction

1-Hydroxybenzotriazole (HOBt) is widely used in peptide synthesis as an activating agent for the acid component and for its ability to suppress racemization. The intermediate benzotriazole active ester **A** then reacts with an amino group to form the urethane bond.^[1] The conversion of **A** into the *N*-oxide isomer **B** was reported.^[2,3]



The *N*-oxide is favored in polar solvents, while the desired active ester **A** predominates in less-polar solvents.^[4] It appears that the active ester **A** is the kinetic product, which is reactive towards rearrangement to the corresponding urethane form **B**.^[5] In addition, Davies et al. proposed the intermediacy of isomer **C** to explain enhanced racemization rates for certain amino acid esters.^[6] Formation of the *N*-oxide under mild conditions was reported by Lu and co-workers by reacting Os_3 clusters with HOBt.^[7] ^{13}C NMR

spectroscopy, used to identify the different isomers, confirmed the predominance of the active ester form **A** in DMSO,^[8] while acetone stabilized the more polar zwitterionic *N*-oxide.^[9] More recently, Carpino reported a detailed investigation into the reactivity of the guanidinium salts HBTU and HATU. It was shown that the *O*-substituted uronium salt is significantly more reactive in peptide coupling reactions than the *N*-substituted guanidinium salt.^[10]

In the context of organometallic peptide conjugates, OBt-active esters provide a convenient route to labeling peptides under very mild conditions, which are also readily automated for solid-phase peptide synthesis (SPPS). This was shown by the use of benzotriazolyl ferrocenecarboxylate as a stoichiometric delivery reagent for the redox active ferrocene (Fc) group, or more recently by the use of one-pot reactions involving cobaltocenium carboxylic acid and TBTU and HATU.^[11] Whether the active ester is used stoichiometrically or used as an intermediate in a one-pot reaction or during SPPS, there is the potential for lowered incorporation of the organometallic label due to different reaction kinetics. During the preparation and column separation of Fc-peptide conjugates, we along with other groups noticed the appearance of a red Fc-containing material, which also appears to possess an OBt substituent. However, it was not possible to properly identify this material. Given that the main role of OBt active ester intermediates is the preparation of organometallic peptide conjugates, we decided to investigate this in more detail. Here we describe our results of the study into the preparation of the OBt active ester **2** of 1'-(*tert*-butyloxycarbonylamino)ferro-

^[a] Department of Chemistry, University of Saskatchewan, 110 Science Place, Saskatoon, SK S7N 5C9, Canada
Fax: (internat.) + 1-306-966-4660
E-mail: kraatz@skyway.usask.ca

^[b] Saskatchewan Structural Science Centre, University of Saskatchewan, Saskatoon, SK S7N 5C9, Canada

cene-1-carboxylic acid and its isomer 3- $\{[1'-(tert\text{-}butyloxy\text{-}carbonylamino)ferrocene\text{-}1\text{-}yl]carbonyl\}$ benzotriazole 1-oxide (3).

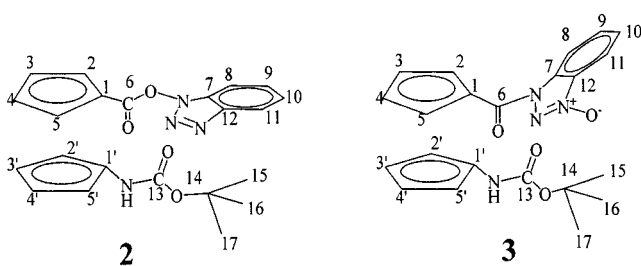
Results and Discussion

During the synthesis of the active ester **2**, from 1'-(*tert*-butoxycarbonylamino)ferrocene-1-carboxylic acid (**1**), in the presence of HOBt and EDC, we prepared and isolated in addition to the desired product **2**, the zwitterionic *N*-oxide **3** (Scheme 1). We have no indication of the formation of the 2-ferrocenylated product.

The two forms are readily separated from each other by chromatography, giving **2** as an orange-red compound and compound **3** as a dark red crystalline compound. The experimental results show that the active ester **2** is the kinetic product, which undergoes rearrangement to the corresponding urethane form.^[5] The rearrangement process is phase dependant; in dry dichloromethane the product **3** is obtained in 4% yield while in aqueous acetone the rearrangement is faster producing 11% yield of **3**. Although, we expected higher reactivity according to earlier reports,^[10] the electron-withdrawing effect of the *N*-oxide group most likely deactivates **3** with respect to its reactivity with the amino acids. Thus, we did not observe any reactivity with glycine.

Compounds **2** and **3** were characterized by NMR spectroscopy ^1H , $^{13}\text{C}\{^1\text{H}\}$, DEPT-135 NMR, HMQC (Heteronuclear Multiple Quantum Correlation), and HMBC (Heteronuclear Multiple Bond Correlation). Table 1 summarizes the complete assignment of the NMR signals for compounds **2** and **3**. It is interesting to note that the signals due to H2, H5 and H2', H5' are observed at significantly different chemical shifts, indicating changes in the local environment due to the change in the substituent, which undoubtedly affects both C rings. Changes are also significant in the ^{13}C chemical shifts of the *ipso*-carbon atoms indicating that electronic differences due to the substituents are "seen" by the Fc system. C1 is affected more by the change from ester to amide *N*-oxide than C1', the *ipso*-C to which the different substituent is attached. Comparing the chemical shifts for the proton H11 in **2** and **3**, this proton is particularly deshielded due to the proximity to the *N*-oxide group in **3**. The NH proton showed broad singlets at $\delta = 6.42$ and 5.75 ppm for **2** and **3**, respectively.

Table 1. Spectroscopic characterization of compounds **2** and **3**

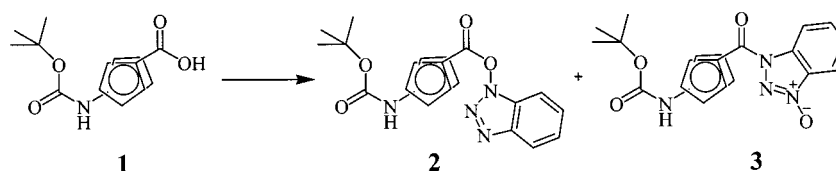


Site	^1H	^{13}C	HMQC	HMBC	^1H	^{13}C	HMQC	HMBC
1'				100.2				98.9
1				65.2				71.6
2', 5'	4.71		62.9		4.52		62.7	
2, 5	5.00		72.3		5.36		74.1	
3', 4'	4.08		55.9		3.94		67.0	
3, 4	4.62		74.7		4.63		74.8	
6		167.5				168.0		
7				129.5				132.4
8	8.02		120.8		7.97		115.7	
9	7.38		125.2		7.49		127.0	
10	7.49		129.1		7.72		133.2	
11	7.45		109.1		8.46		117.3	
12				143.9				133.82
13		153.5				153.5		
14				80.6				80.5
15–17	1.27		28.5		1.26		28.5	

Both compounds exhibit a single broad absorbance in the visible region. For compound **2**, $\lambda_{\text{max.}} = 453$ nm, while for **3** the band is observed at $\lambda_{\text{max.}} = 484$ nm. This bathochromic shift clearly shows electronic coupling of the *N*-oxide OBt with the Fc group. Shifts were also observed for pyridine *N*-oxides (305–333 nm) and quinoline *N*-oxides (> 320 nm) with substituents that are in direct conjugation with the *N*-oxide group, and rationalized in terms of tautomer and resonance contributions. In quinoxaline di-*N,N*-oxide shifts are due to intramolecular charge transfer.^[12]

The IR spectra of both compounds show two carbonyl bands. For compound **2** a band due to the active ester is observed at 1788 cm^{-1} . This band is absent in compound **3** and is replaced by an amide band at 1688 cm^{-1} . Both compounds exhibit a strong absorption around 1722 cm^{-1} , due to the carbamate carbonyl group on the other Cp ring.

Crystal Structures of 2 and 3: Selected bond lengths and angles for **2** and **3** are given in Table 2. ORTEP views of



Scheme 1

Table 2. Relevant bond lengths (Å) and angles (°) for **2** and **3**

	2	3
av. Fe(1)–C(Cp1)	2.038(14)	2.039(13)
av. Fe(1)–C(Cp2)	2.043(16)	2.047(12)
C(10)–C(15A)/C(10)–C(15A)	1.489(9)	1.459(2)
C(15A)–O(11A)/C(15)–O(11)	1.172(9)	1.210(2)
C(15A)–O(12A)/C(15)–N(11)	1.429(8)	1.426(2)
O(12A)–N(11)	1.358(3)	
N(11)–N(12)	1.342(2)	1.364(2)
N(12)–N(13)	1.302(4)	1.308(2)
N(13)–O(12)		1.2699(19)
C(20)–N(21)	1.411(4)	1.401(2)
N(21)–C(25)	1.349(4)	1.366(2)
C(25)–O(22)	1.350(3)	1.348(2)
C(25)–O(21)	1.207(3)	1.206(2)
C(10)–C(15A)–O(12A)/C(10)–C(15)–N(11)	106.6(6)	119.2(1)
C(10)–C(15)–O(11A)/C(10)–C(15)–O(11)	131.7(6)	125.4(2)
C(20)–N(21)–C(25)	123.7(2)	124.9(1)
N(11)–N(12)–N(13)	106.4(3)	105.5(1)
N(21)–C(25)–O(22)	109.6(2)	107.3(1)
N(21)–C(25)–O(21)	124.8(3)	126.0(1)

these complexes are presented in Figures 1 and 2, respectively.

Compound **2** crystallizes in the polar orthorhombic space group $Pna2_1$ as a twinned racemic crystal, whereas compound **3** crystallizes in the monoclinic space group $P2_1/c$. In both complexes, the Cp rings are virtually parallel to each other [Cp–Fe–Cp angles: **2**: 2.1(3)°; **3**: 2.98(14)°]. The distances of the Fe atoms to the carbon atoms of the Cp rings are in the expected range in comparison to other ferrocene structures.^[13]

For compound **2**, the bond lengths and angles of the Cp-ester-benzotriazole moiety are almost identical to those reported for Fc–CO–OBt.^[14,15] The ester bond to the benzotriazole moiety in **2** is long [1.429(8) Å], as expected. The benzotriazole (Bt) substituent is rotated out of the ester plane by only 80.8(2)°, compared to 96.56(6)° in Fc–CO–OBt.^[15] In the case of Fc–CO–OBt, this does not permit the efficient interaction between the two π -systems,^[15] but increases reactivity of the carbonyl C atom towards external nucleophiles and therefore allows a faster reaction of the ester. A similar observation was made for (*S*)-3-(*O* γ -methyl,*N* α -triphenylmethylglutamyl)benzotriazole 1-oxide,^[16] which bears the acyl and OBt groups on the same plane, resulting in a slower reactivity towards amines compared to the OBt active ester.^[17] 3-(*N* α -Tritylmethylthionyl)benzotriazole 1-oxide also exhibits the same structural features with coplanar OBt and acyl groups.^[18] The geometry and conformation for a variety of ester and amide derivatives of HOBt and HOAt have been reported.^[19,20] A more recent investigation into the reactivity of HATU showed that the *O*-substituted uronium salt is significantly more reactive in peptide coupling reactions than the *N*-substituted guanidinium salt,^[10] in line with earlier investigations on OBt derivatives. In compound **3**, the planar OBt *N*-oxide, the urethane and the Cp ring to which it is at-

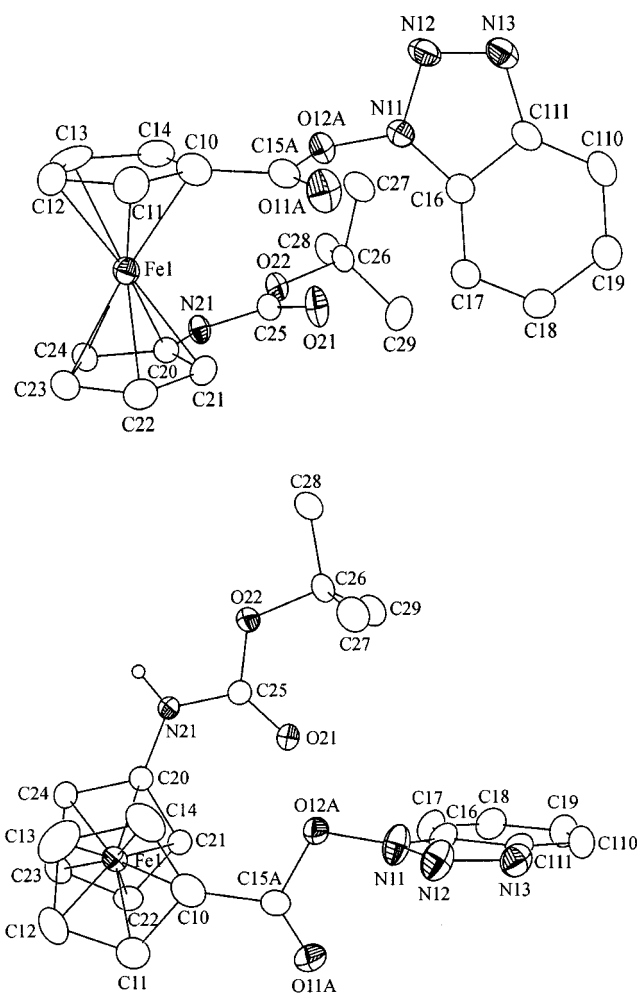


Figure 1. ORTEP drawing of compound **2** (30% probability); H atoms omitted for clarity; side-on view and view down the Cp–Fe–Cp axis to visualize the 1,2'-conformation of the Fc group

tached are not coplanar [OBt *N*-oxide/Cp, 16.5(1)°; amide/Cp, 18.9(1)°]. Just like the parent benzotriazole-1-oxide and hydroxybenzotriazole, the heterocycle in compound **3** is essentially flat. In the *N*-oxide, the N–N bond lengths are shortened compared to hydroxybenzotriazole. For compound **3**, the N–N bond lengths in the heterocycle are non-equidistant. The distance between the N(O)–N are shorter and the distance N(12)–N(13) of 1.3084(19) Å indicates significant double bond character between the two nitrogen atoms. Similar observations were made have been made for (*S*)-3-(*O* γ -methyl,*N* α -triphenylmethylglutamyl)benzotriazole 1-oxide and 3-(*N* α -tritylmethylthionyl)benzotriazole 1-oxide. As seen from Table 3, the urethane moieties in **2** and **3** are not coplanar with the Cp rings. The observed ω angle for **2** is close to the ideal value for a 1,2' conformation (–72°), while **3** crystallizes in the 1,1'-conformation with $\omega = 13.3(8)$ °.

There is no hydrogen bonding present between adjacent molecules of **2**. The amide proton does not point towards the Bt substituent. In contrast, hydrogen bonding is observed in the structure of compound **3** between the oxygen

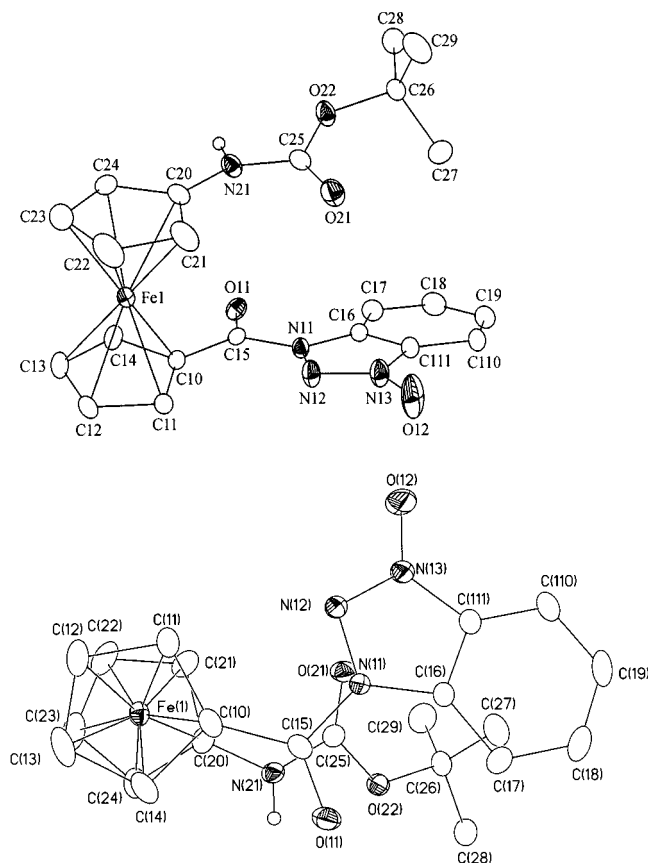


Figure 2. ORTEP drawing of compound **3** (30% probability); H atoms omitted for clarity; side-view and view down the Cp–Fe axis to show the 1,1'-conformation of the Fc system

Table 3. Torsions angles (°) for **2** and **3**

Angle	2	3
$\theta^{[a]}$	2.1(3)	2.98(14)
$\beta^{[b]}$	5.0(7) [C(<i>ipso</i>)–C=O] / 12.3(2) [N–C=O]	18.8(2) [C(<i>ipso</i>)–C=O] / 18.9(1) [N–C=O]
$\omega^{[c]}$	–70.8(8)	13.3(8)

^[a] The dihedral angle between two Cp rings. ^[b] The dihedral angle between the plane of the Cp ring and the C(*ipso*)C=O bond or between the plane of the Cp ring and the N–C=O bond. ^[c] The torsion angle is defined as C(*ipso*)–Cp(centroid)–C(*ipso*).

atom attached to one of the nitrogen atoms of the Bt substituent, carrying a partial negative charge, and the amide proton in an adjacent molecule. The O(12)⋯N(21)^{*} bond lengths of 2.859(2) Å indicates the presence of strong hydrogen bonding in the solid state.

The packing arrangements in **2** and **3** are very different (Figure 3). In compound **3**, the Fc groups are aligned with the NO groups of the Bt group in the adjacent molecules forming strands along the *c*-axis. In **2**, the molecules form a strand-like arrangement along the 2₁-axis with the Fc groups adjacent to each other.

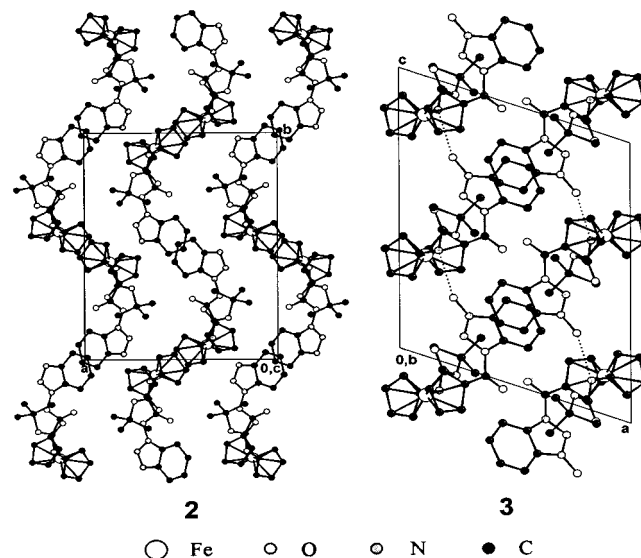


Figure 3. Packing diagrams for compounds **2** and **3**

Heinze recently^[14] reported the structural properties of the acetamino-analogue of compound **2**. In the solid state, the molecule displayed significant intramolecular hydrogen bonding. The Boc derivative **2** on the other hand, does not display any intramolecular hydrogen bonding involving the urethane NH group. Compound **3** on the other hand displays intermolecular hydrogen bonding in the solid state. This raises the question whether the presence of the Boc-

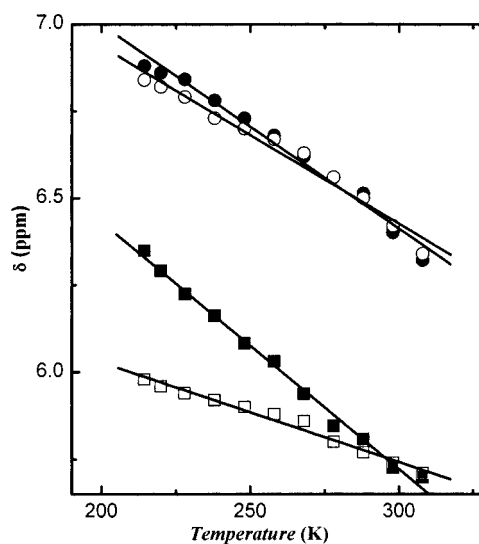


Figure 4. Temperature dependence of the chemical shifts for NH signals of compounds **2** (circles), **3** (squares) in CDCl₃ [open symbols indicate 1 mM; solid symbols indicate 50 mM]

protecting group can account for the differences in H-bonding behavior in the solid-state structures. Is the lack of intramolecular hydrogen bonding in compound **2** due to the spatial requirement of the bulky Boc carbamate group? In order to answer these questions, we decided to investigate the hydrogen-bonding behavior of compounds **2** and **3** in solution. Variable-temperature ^1H NMR studies of compounds **2** and **3**, recorded at 1 and 50 mM in CDCl_3 in the temperature range 215 and 308 K, showed a significant difference in the NH chemical shift between the two compounds with the temperature variation. A plot of $\Delta\delta$ versus T is shown in Figure 4. For compound **2**, the chemical shift of the amide NH was affected by temperature but the temperature dependence was independent of concentration (1 mM: -5.1 ppb K^{-1} ; 50 mM: -6.4 ppb K^{-1}).

In contrast, compound **3** displayed a concentration dependent temperature behavior (1 mM: -2.8 ppb K^{-1} ;

50 mM: -7.1 ppb K^{-1}), indicating the presence of intermolecular hydrogen bonding in compound **3** in solution. The temperature behavior of the NH chemical shift indicates the presence of intramolecular hydrogen bonding in compound **2** in solution.^[11,21] However, the crystal structure does not show any hydrogen bonding, presumably as a result of crystal packing. Interestingly, the Cp protons in compound **2** undergo some temperature dependent changes, as is shown in Figure 5. The signals due to H2 and H5 in compound **2** are very broad at low temperatures (215–220 K) but appear at 228 K, and gradually sharpen. Heinze's Ac derivative displays a similar temperature behavior, which was interpreted as a possible interconversion between two ferrocenyl rotamers of the molecule. Our results suggest that a similar equilibrium may also exist for compound **2**. The Cp region of compound **3** does not change with temperature (Figure 6).

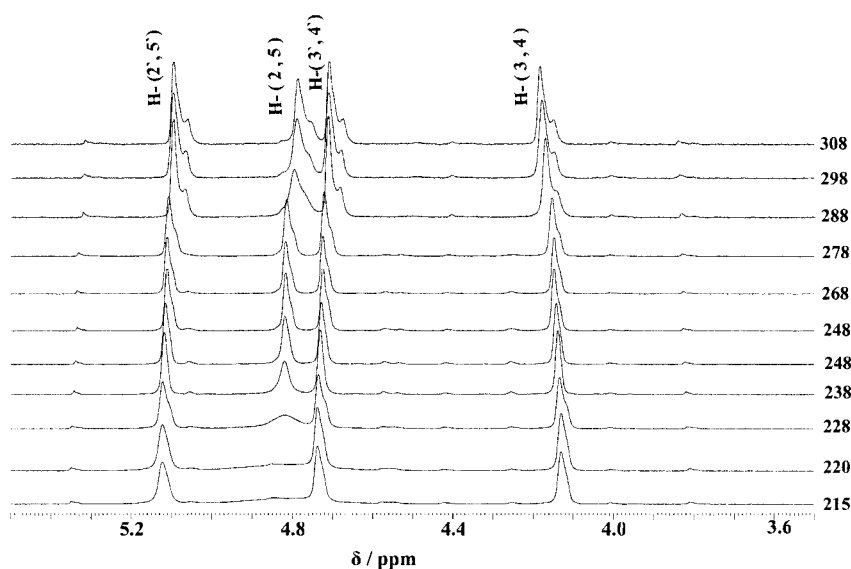


Figure 5. Variable temperature ^1H NMR spectra of **2** (50 mM, CHCl_3) in a region of 215–308 K

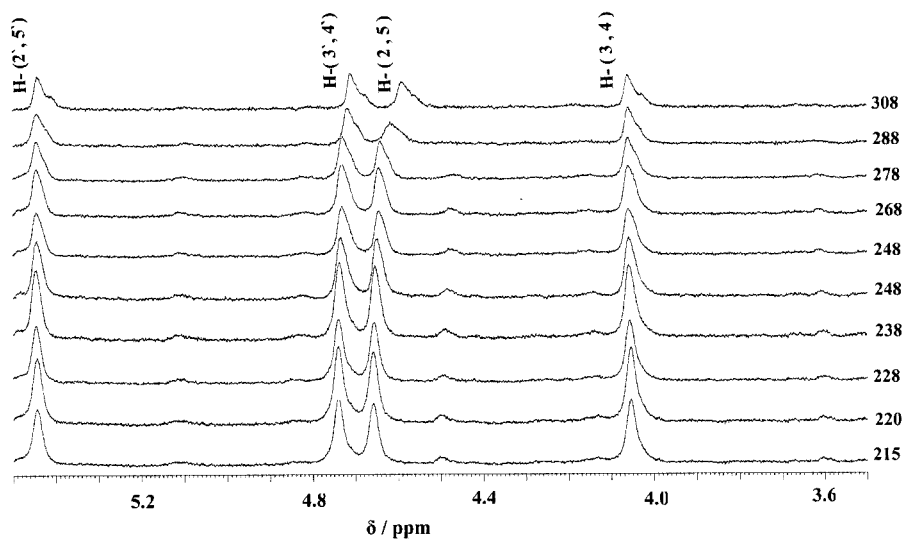


Figure 6. Variable temperature ^1H NMR spectra of **3** (50 mM, CHCl_3) in a region of 215–308 K

Figure 7 shows the electrochemical behavior of compounds **2** and **3**. Both compounds show a quasi-reversible single one-electron oxidation. The separation between oxidative and reductive peak potentials ΔE_p is about 96 ± 5 mV for **2** (87 ± 5 mV for **3**). The ratio of peak currents is close to unity for both compounds (**2**: $i_c/i_a = 1$; **3**: $i_c/i_a = 1.05$). As expected for *N*- and *O*-ferrocenylated systems, the halfwave potentials $E_{1/2}$ for **2** and **3** are significantly different. While $E_{1/2} = 672 \pm 5$ mV for the active ester **2**, the $E_{1/2} = 591 \pm 5$ mV for the *N*-oxide **3**.

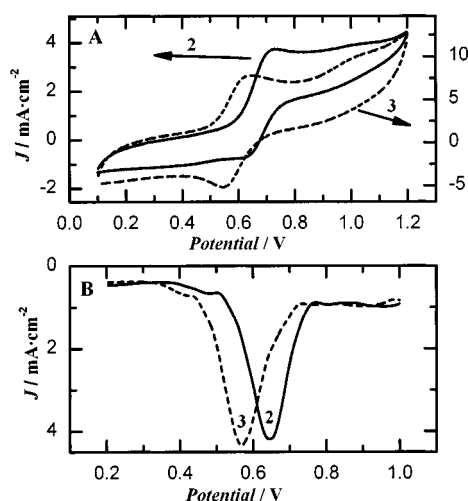


Figure 7. Electrochemical study of compounds **2** and **3** in $\text{CH}_3\text{CN}/0.1$ M TBAP: **A** shows the cyclic voltammetry at a scan rate of 100 mV/s (ΔE_p for the Fc/Fc^+ couple under identical conditions was 68 ± 5 mV); **B** shows the differential pulse voltammetry at a scan rate 10 mV/s; for **2**: DPV, $E_p = 643 \pm 5$ mV; for **3**, $E_p = 566 \pm 5$ mV

Conclusion

In summary, we have prepared the two ferrocene-amino acid derivatives **2** and **3** and report their full characterization. Initially, compound **3** was obtained as a by-product in the preparation of the desired active ester. Reports on HATU active esters show this to be a common reaction in peptide synthesis. Importantly, this by-product was not reported in ferrocene chemistry. Given the importance of the Fc-OBt active ester intermediates in the preparation of Fc-bioconjugates and as a potential intermediate for the stepwise synthesis of ferrocenamide-based polymers, our finding is significant. Importantly, the reactivity towards peptide coupling is different. Whereas, the active ester derivative **2** undergoes amide bond formation with glycine ethyl ester and other amino acids and peptides,^[22] the *N*-oxide **3** does not react. This is in contrast with earlier reports on the reactivity of HATU *N*-oxide derivatives, which were shown to undergo a slow conversion into the desired amide.

Experimental Section

General Procedure: The syntheses of 1'-(*tert*-butyloxycarbonylamino)ferrocene-1-carboxylic acid (**1**) was carried out using the pub-

lished procedure.^[23] All syntheses were carried out in air unless otherwise indicated. CH_2Cl_2 (BDH; ACS grade) used for synthesis was dried (CaH_2) and distilled prior to use. CDCl_3 (Aldrich) was dried (CaH_2), and stored over molecular sieves (8–12 mesh; 4 Å effective pore size; Fisher) before use. EDC·HCl, HOBt (Quantum), MgSO_4 , and NaHCO_3 (VWR) were used as received. For column chromatography, a column with a width of 2.7 cm (ID) and a length of 45 cm was packed 18–22 cm high with 230–400 mesh silica gel (VWR). For TLC, aluminum plates coated with silica gel 60 F_{254} (EM Science) were used. NMR spectra were recorded with a Bruker Avance-500 spectrometer using a 5-mm broadband probe operating at 500.134 MHz (^1H) and 125.766 MHz ($^{13}\text{C}\{^1\text{H}\}$). Peak positions in both ^1H and ^{13}C spectra are reported in ppm relative to TMS. The ^1H NMR spectra are referenced to the residual CHCl_3 signal at δ 7.27. All $^{13}\text{C}\{^1\text{H}\}$ spectra are referenced to the CDCl_3 signal at δ = 77.23 ppm. Mass spectrometry was carried out with a VG Analytical 70/20 VSE instrument. Infrared spectra were obtained with a Perkin–Elmer model 1605 FT-IR.

Preparation of (Benzotriazol-1-yl) 1'-(*tert*-Butyloxycarbonylamino)-ferrocene-1-carboxylate (2**) and 3-[[1'-(*tert*-Butyloxycarbonylamino)ferrocene-1-yl]carbonyl]benzotriazole 1-Oxide (**3**). **Procedure A:** Solid HOBt (4.05 mmol, 0.62 g) and EDC·HCl (4.05 mmol, 0.78 g) were added to a solution of 1'-(*tert*-butyloxycarbonylamino)-ferrocene-1-carboxylic acid (**1**) (3.68 mmol, 1.27 g) in CH_2Cl_2 (40 mL). The reaction mixture was stirred at room temperature (20 °C) for 2 h and then treated with an aqueous solution of saturated NaHCO_3 , citric acid (10%), and water. The organic phase was separated and dried with Na_2SO_4 , and evaporated to dryness under reduced pressure. The crude product was purified by flash column chromatography (SiO_2 , $\text{EtOAc}/\text{hexanes}$, 1:2) to give dark orange crystals of compound **2** (1.32 g, 78%) (R_f = 0.74), followed by red crystals of compound **3** (68 mg, 4%) (R_f = 0.42). **Procedure B:** The same mixture as described under **A** was stirred at room temperature for two hours in aqueous acetone (30 mL). The reaction mixture was dried under reduced pressure and redissolved in CH_2Cl_2 . After the purification (vide supra), compounds **2** and **3** were obtained in yields of (1.15 g, 64%) and (180 mg, 11%), respectively.**

Characterization of 2: FAB-MS (m/z): calcd. for $\text{C}_{22}\text{H}_{22}\text{FeN}_4\text{O}_4$ [$M + 1$] $^+$: 463.2; found 463.1. FT-IR (KBr (cm^{-1})): $\tilde{\nu}$ = 3322 (m, N–H), 1788, 1723 (s, C=O). UV/Vis (MeCN): λ (ϵ , $\text{L}\cdot\text{mol}^{-1}\cdot\text{cm}^{-1}$) = 453 nm (706). ^1H NMR (CDCl_3): δ = 8.02 (d, $J_{\text{H,H}}$ = 8.5 Hz, 1 H, *Bt*-ArH), 7.49 (t, $J_{\text{H,H}}$ = 15.0 Hz, 1 H, *Bt*-ArH), 7.45 (d, $J_{\text{H,H}}$ = 8.2 Hz, 1 H, *Bt*-ArH), 7.38 (t, $J_{\text{H,H}}$ = 15.2 Hz, 1 H, *Bt*-ArH), 6.42 (br. s, 1 H, NH), 5.00 (s, 2 H, H-2 and H-5, Fc), 4.71 (s, 2 H, H-2' and H-5', Fc), 4.62 (s, 2 H, H-3 and H-4, Fc), 4.08 (s, 2 H, H-3' and H-4', Fc), 1.27 [s, 9 H, $\text{C}(\text{CH}_3)_3$] ppm. $^{13}\text{C}\{^1\text{H}\}$ NMR (CDCl_3): δ = 167.5 (s, COON-Bt), 153.5 [s, $\text{COOC}(\text{CH}_3)_3$], 143.9, 129.5 (quaternary C of Ar Bt), 129.1, 125.2, 120.8, 109.1 (s, Ar Bt), 100.2 (C-1', Fc), 80.58 [$\text{C}(\text{CH}_3)_3$], 74.7 (C-3 and C-4, Fc), 72.3 (C-2 and C-5, Fc), 66.9 (C-3' and C-4', Fc), 65.2 (C-1, Fc), 62.3 (C-2' and C-5', Fc), 28.5 [$\text{C}(\text{CH}_3)_3$] ppm.

Characterization of 3: FAB-MS (m/z): calcd. for $\text{C}_{22}\text{H}_{22}\text{FeN}_4\text{O}_4$ [$M + 1$] $^+$: 463.2; found 463.1. FT-IR (KBr (cm^{-1})): $\tilde{\nu}$ = 3310 (m, N–H), 1721, 1688 (s, C=O). UV/Vis (MeCN): λ (ϵ , $\text{L}\cdot\text{mol}^{-1}\cdot\text{cm}^{-1}$) = 484 nm (1200). ^1H NMR (CDCl_3): δ = 8.46 (d, $J_{\text{H,H}}$ = 8.5 Hz, 1 H, *Bt*-ArH), 7.97 (d, $J_{\text{H,H}}$ = 8.4 Hz, 1 H, *Bt*-ArH), 7.72 (t, $J_{\text{H,H}}$ = 15.5 Hz, 1 H, *Bt*-ArH), 7.49 (t, $J_{\text{H,H}}$ = 17.3 Hz, 1 H, *Bt*-ArH), 5.75 (br. s, 1 H, NH), 5.36 (s, 2 H, H-2 and H-5, Fc), 4.63 (s, 2 H, H-3 and H-4, Fc), 4.52 (s, 2 H, H-2' and H-5', Fc), 3.94 (s, 2 H, H-3' and H-4', Fc), 1.26 [s, 9 H, $\text{C}(\text{CH}_3)_3$] ppm. $^{13}\text{C}\{^1\text{H}\}$ NMR (CDCl_3): δ = 168.0 (s, CON-Bt), 153.5 [s, $\text{COO}(\text{CH}_3)_3$], 133.8, 132.4 (quaternary C of Ar Bt), 133.2, 127.0,

Table 4. X-ray crystallographic data of complexes **2** and **3**

	2	3
Formula	C ₂₂ H ₂₂ FeN ₄ O ₄	C ₂₂ H ₂₂ FeN ₄ O ₄
Molecular mass	462.29	462.29
Crystal dimensions (mm)	0.15 × 0.15 × 0.10	0.25 × 0.20 × 0.13
Crystal system	Orthorhombic	monoclinic
Space group (no.)	<i>Pna</i> 2 ₁	<i>P</i> 2 ₁ / <i>c</i> (14)
<i>a</i> (Å)	12.6580(2)	11.8140(2)
<i>b</i> (Å)	17.2760(3)	12.0982(2)
<i>c</i> (Å)	9.7170(5)	15.4850(3)
β (Å)	90	110.9844(8)
Cell volume (Å ³)	2124.91(2)	2066.45(6)
Molecular units per cell	4	4
μ (mm ⁻¹)	0.746	0.768
Density (calcd.) (g·cm ⁻³)	1.445	1.486
<i>T</i> (K)	173	173
Scan range (2 θ)	1.99–24.70	3.28–30.06
Scan speed (s frame ⁻¹)	135	40
Measured reflections	3462	11239
Unique reflections	3462	6005
Obsd. reflections (<i>I</i> = 2 σ)	3187	4632
Parameters refined	312	286
Max. residual electron density (Å ⁻³)	0.297 / -0.211	0.357/-0.374
Agreement factors ^[a] (<i>F</i> ² refinement)	<i>R</i> ₁ = 3.27%; <i>R</i> _w = 6.87%	<i>R</i> ₁ = 3.90%; <i>R</i> _w = 9.05%

^[a] $R_1 = [\sum |F_o| - |F_c|] / [\sum |F_o|]$ for $[I > 2\sigma(I)]$. ^[b] $wR_2 = \{[\sum w(F_o^2 - F_c^2)^2] / [\sum w(F_o^2)^2]\}^{1/2}$.

117.3, 115.7 (Ar Bt), 98.9 (C-1', Fc), 80.5 [C(CH₃)₃], 74.8 (C-3 and C-4, Fc), 74.1 (C-2 and C-5, Fc), 71.6 (C-1, Fc), 67.0 (C-3' and C-4', Fc), 62.7 (C-2' and C-5', Fc), 28.5 [C(CH₃)₃] ppm.

Attempted Coupling of **3:** A solution of H-Gly-OEt·HCl (0.24 mmol, 0.03 g) and Et₃N (0.4 mL) in dry CH₂Cl₂ (5 mL) was added to a stirring solution of **3** (0.22 mmol, 0.10 g) in dry CH₂Cl₂ (10 mL). The progress of the reaction was followed by TLC (EtOAc/hexanes/MeOH, 4:5:1). No product was observed after 24 h.

Electrochemical Measurements: The electrochemical experiments were carried out at room temperature using a CV-50 W voltammetric analyzer. A gold electrode (diameter 50 μ m) was used as working electrode. 1 mM solutions of compounds **2** and **3** were prepared in 0.1 M tetrabutylammonium perchlorate (TBAP) solution in a CH₃CN. The measurements carried out at a low scan rate of 100, 10 mV/s for cyclic voltammetry (CV) and differential pulse voltammetry (DPV), respectively. A platinum wire (1 mm) was used as the counter electrode and a Ag/AgCl (BAS) was used as the reference electrode. The *E*_{1/2} of the Fc/Fc⁺ couple under the experimental conditions is 448(±5) mV (vs. Ag/AgCl).

X-ray Crystallography: Suitable crystals of compounds **2** (orange plate-like crystal; 0.15 × 0.15 × 0.10 mm) were obtained from an ether-layered solution of the compounds in chloroform, while **3** (dark red plate-like crystal; 0.25 × 0.20 × 0.13 mm) was obtained by slow evaporation from an ethyl acetate/hexane(3:1) solvent mixture. All measurements were made with a Nonius KappaCCD 4-Circle Kappa FR540C diffractometer using graphite-monochromated Mo-*K*_α radiation (λ = 0.71073 Å) at -100 °C. An initial orientation matrix and cell was determined from 10 frames using ϕ scans.^[24] Data were measured using ϕ - and ω -scans.^[24] The data were processed using the standard Nonius software.^[25] The structures were solved by direct methods (**2**: SIR-97; **3**: SHELXS-97)^[26,27] and refined by full-matrix least-squares methods on *F*² with SHELXL-97-2.^[28] The non-hydrogen atoms were refined an-

isotropically. Hydrogen atoms were included at geometrically idealized positions (C–H bond lengths 0.95/0.99 Å; N–H bond lengths 0.88 Å) and were not refined. The isotropic thermal parameters of the hydrogen atoms were fixed at 1.2 times that of the preceding carbon or nitrogen atom. The carbon and oxygen atoms of one –C(O)O unit [labeled as C(15A), O(11A), O(12A), C(15B), O(11B), O(12B)] in **2** were disordered over two positions with site occupancy factors of 0.825(5) and 0.175(5). The refined absolute structure parameter [0.552(18)] for **2** was neither unity nor nil and was used as the scale parameter in the racemic twin refinement. The hydrogen atom at nitrogen atom N(21) in **3** was located from the Fourier difference map. Its coordinates were allowed to refine, whereas its isotropic thermal parameter was fixed at 1.2 times that of the preceding nitrogen atom. Data relating to the structure determination are presented in Table 4. CCDC-241248 (**2**), -236850 (**3**) contains the supplementary crystallographic data for this paper. These data can be obtained free of charge at www.ccdc.cam.ac.uk/conts/retrieving.html [or from the Cambridge Crystallographic Data Centre, 12 Union Road, Cambridge CB2 1EZ, UK; Fax: (internat.) + 44-1223-336-033; E-mail: deposit@ccdc.cam.ac.uk].

Acknowledgments

Financial support from NSERC, CFI and SIF is gratefully acknowledged. H.-B. K. is the Canada Research Chair in Biomaterials. We are grateful to the Saskatchewan Structure Science Center (SSSC) for providing access to all necessary instrumentation. Ken Thoms, Department of Chemistry, University of Saskatchewan, is also acknowledged for carrying out the MS experiments.

^[1] W. König, R. Geiger, *Chem. Ber.* **1970**, *103*, 788.

^[2] S. I. Murahashi, H. Mitsui, T. Watanabe, S. I. Zenki, *Tetrahedron Lett.* **1983**, *24*, 1049.

- [3] R. Bosch, G. Jung, W. Winter, *Acta Chyst.* **1983**, C39, 1089.
- [4] F. T. Boyle, R. A. Y. Jones, *J. Chem. Soc., Perkin Trans.* **1973**, 2, 160.
- [5] J. Singh, R. Fox, M. Wong, T. P. Kissick, J. I. Moniot, *J. Org. Chem.* **1988**, 53, 205.
- [6] J. S. Davies, A. K. Mohammed, *J. Chem. Soc., Perkin Trans.* **1981**, 1, 2982.
- [7] K. Lu, S. Kumaresan, Y. Wen, J. R. Hwu, *Organometallics* **1994**, 13, 3170.
- [8] F. Alain, J. Elguero, A. F. Hegarty, D. G. McCarthy, *Org. Magn. Reson.* **1980**, 13, 339.
- [9] E. Anders, A. R. Katritzky, N. Malhotra, J. Stevens, *J. Org. Chem.* **1992**, 57, 3698.
- [10] L. A. Carpino, H. Imazumi, A. El-Faham, *Angew. Chem. Int. Ed.* **2002**, 41, 441.
- [11] D. R. v. Staveren, T. Weyhermuller, N. Metzler-Nolte, *Dalton Trans.* **2003**, 210.
- [12] V. P. Andreev, A. V. Ryzhakov, *Khim. Geterotsikl. Soedin.* **1993**, 12, 1662.
- [13] T. Okamura, K. Sakauye, N. Ueyama, A. Nakamura, *Inorg. Chem.* **1998**, 37, 6731.
- [14] K. Heinze, M. Schlenker, *Eur. J. Inorg. Chem.* **2004**, 2053.
- [15] H.-B. Kraatz, J. Lusztyk, G. D. Enright, *Inorg. Chem.* **1997**, 36, 2400.
- [16] P. Mamos, D. Papaioannou, C. Kavounis, V. Nastopoulos, *Acta Crystallogr., Sect. B* **1997**, 53, 1973.
- [17] K. Barlos, D. Papaioannou, D. Theodoropoulos, *Int. J. Peptide Protein Res.* **1984**, 23, 300.
- [18] K. Barlos, D. Papaioannou, S. Voliotis, R. Prewo, J. Bieri, *J. Org. Chem.* **1985**, 50, 696.
- [19] M. Crisma, G. Valle, V. Moretto, F. Formaggio, C. Toniolo, *Lett. Pept. Sci.* **1998**, 5, 247.
- [20] C. Toniolo, M. Crisma, F. Formaggio, *Biopolymers (Pept. Sci.)* **1996**, 40, 627.
- [21] E. S. Stevens, N. Sugawara, G. M. Bonora, C. Toniolo, *J. Am. Chem. Soc.* **1980**, 102, 7048.
- [22] N. Metzler-Nolte, private communication.
- [23] L. Barisic, V. Kovac, *Croat. Chem. Acta* **2002**, 75, 199.
- [24] COLLECT data collection software, N. B.V., **1998**.
- [25] H. D. SCALEPACK, W. M. v1.96: Z. Otwinowski, *Processing of X-ray Diffraction Data Collected in Oscillation Mode, Methods in Enzymology*, vol. 276 (Macromolecular Crystallography, part A) (Eds.: C. W. Carter, Jr., R. M., Sweet); Academic Press, San Diego, CA, **1997**.
- [26] A. Alatomare, M. C. Burla, M. Camalli, G. L. Casciarano, C. Giacovazzo, A. Guagliardi, A. G. G. Moliterni, G. Polidori, R. Spagna, *J. Appl. Crystallogr.* **1999**, 32, 115.
- [27] G. M. Sheldrick, *SHELXS-97*, University of Göttingen, Göttingen, Germany, **1997**.
- [28] G. M. Sheldrick, Program for the Solution of Crystal Structures; University of Göttingen, Göttingen, Germany, **1997**.

Received June 10, 2004

Early View Article

Published Online November 10, 2004